Journal of Theoretical and Applied Mechanics, Sofia, 2012, vol. 42, No. 1, pp. 71–90

FLUID MECHANICS

SOLAR WIND-COMET EXOSPHERE INTERACTION. 2. COULD THE SINGLE-FLUID GAS-DYNAMIC MODEL BE APPLICABLE TO THE ROSETTA MISSION*

M. Kartalev, P. Dobreva, V. Keremidarska
Institute of Mechanics, Bulgarian Academy of Sciences,
Acad. G. Bonchev St., Bl. 4, 1113 Sofia, Bulgaria,
Geospace Modeling and Forecasting Center –
Institute of Mechanics, GIS Foundation, Sofia Bulgaria,
e-mails: m_kartalev@yahoo.com, polya2006@yahoo.com

M. Dryer
Center for Space Plasma and Aeronomic Research,
University of Alabama in Huntsville, Huntsville, AL, 35899, USA
e-mail: murraydryer@msn.com

[Received 24 August 2011. Accepted 03 October 2011]

Abstract. The capabilities of a single fluid gasdynamic model of solar wind-comet exosphere interaction, presented in the accompanying (Keremidarska et al.) [23], are discussed from the point of view of its potential implementation in interpreting data, expected to be obtained by ROSETTA mission instruments in plasma environments of the comet 67P/Churyumov-Gerasimenko. As an exapmle, some model's predictions of the structure and parameters' distribution in the inner coma of P/Halley are presented and compared with Giotto measurements. Special attention is paid to a possible non-traditional interpretation of the magnetic cavity boundasry, registered by Giotto magnetometer. Possible model's applications are discussed for each of the main expected stages in the evolution of the comet 76P/CG environments during ROSETTA rendezvous with the comet.
Key words: Comet, gas-dynamics, numerical modelling, Rosetta mission.

*Corresponding author e-mail: polya2006@yahoo.com

This work is supported by the European Social Fund and Bulgarian Ministry of Education, Youth and Science under Operative Program "Human Resources Development", Grant BG051PO001-3.3.04/40. This research was also partially supported by the Bulgarian National Council Scientific Research under project NZ-1315/03. MK were supported by the Air Force Office of Scientific Research, Air Force Material Command, USAF, under grant FA8655-05-1-3024.

1. Introduction

The ESA ROSETTA space mission [12] has been launched to make a rendezvous with the short period comet 67P/Churyumov-Gerasimenko (67P/CG) and to study it from about 3.25 AU to perihelion and up to 2 AU postperihelion, thus providing a unique opportunity to monitor its behaviour over a wide range of distances from the Sun. (The Astronomical Unit (AU) is equal to about 149,597,870.7 kilometers.) This is a typical Jupiter-Family comet with a perihelion distance of 1.3 AU and a maximum expected gas production rate in the vicinity of 5×10^{27} s^{-1}.

ESA's Rosetta spacecraft will be the first one to undertake the long-term exploration of a comet at close quarters. It comprises a large orbiter, which is designed to operate for a decade at large distances from the Sun, and a small lander. Each of these carries a large complement of scientific experiments, designed to complete the most detailed study of a comet ever attempted. The spacecraft will release a small lander onto the icy nucleus, after entering orbit around Comet 67P/Churyumov-Gerasimenko in 2014, then will spend the next two years orbiting the comet as it heads towards the Sun.

Our interest in this mission is focused on the possible model interpretations of the expected measurements of the instruments of the the Rosetta Plasma Consortium [31]. Plasma and wave package, Rosetta Plasma Consortium, RPC, is a part of the Rosetta orbiter payload. RPC is a highly integrated package that consists of five sensors: the Langmuir Probe, LAP, the Ion and Electron Sensor, IES, the Ion Composition Analyzer, ICA, the Fluxgate Magnetometer, MAG, and the Mutual Impedance Probe, MIP. The prime objectives of RPC are to investigate: (1) the physical properties of the cometary nucleus and its surface, (2) the inner coma structure, dynamics, and aeronomy, (3) the development of cometary activity, and the microscopic and macroscopic structure of the solar-wind interaction region. The scientific goal of the RPC is to study the interaction of the magnetized solar wind plasma with comet 67P/Churyumov-Gerasimenko during its approach to the Sun, that means to study the evolution of the interaction region during increasing cometary activity. Two basically **different modes** of this interaction are expected to be discriminated (e.g. [13]):

Mode 1 Interaction of the inactive cometary nucleus.

Mode 2 Interaction of the active nucleus with the magnetized interplanetary medium.

Special efforts in the literature are recently directed in preparation solar wind-comet interaction models, adequately describing possible expected cases

of this interaction, respectively. Thus, Hansen et al. (2007) [15] have chosen to model the comet at four representative heliocentric radial distances that represent either significant times of the mission or serve to span the range of plasma environments, that can be expected during the mission. These authors applied in this modelling both a fluid-based magnetohydrodynamic (MHD) model, as well as a semi-kinetic hybrid particle model to study the plasma distribution. They found that near perihelion the interaction is well described by a fluid picture, where a bow shock and diamagnetic cavity are formed (supposing that the diamagnetic cavity is equivalent to the contact surface in the Fig. 1 of [23]). Near the beginning of the Rosetta comet encounter the low production rate results in an interaction that only very slightly perturbs the solar wind. Near perihelion, the plasma environment displays a scaled-down version of the "classical" fluid result seen by the Giotto spacecraft at comet Halley.

In the present paper, we demonstrate and justify on the example of Giotto's measurements near Comet Halley the capabilities of the much simpler one-fluid gas-dynamic approach to predict the observed interaction picture and parameters' distribution – especially in the inner coma. In the accompanying paper Keremidarska et al. (2011) [23] we describe in details a single-fluid gas-dynamic numerical approach in modelling the solar wind interaction with a comet exosphere. Several essential source and sink processes are taken into account in the considered model. The introduced appropriate right hand terms in the Euler gasdynamic equations correspond to the processes: photoionization, charge transfer, impact ionization, ion-neutral chemical reactions, other than charge-transfer - such as atom-atom interchange, dissociative recombination, ion-neutral frictional force. Some details of the utilized grid-characteristics numerical scheme, developed by Zapryanov and Minostsev (1964) [33] and Magomedov and Holodov (1988) [25], are also exposed in the [23]. This scheme has been already applied quite extensively (with zero right-hand sides of the Euler equations) in modelling the solar wind-Earth's magnetosphere interaction Kartalev et al.(1996, 2002, 2006, 2008) [16, 20, 21, 22], Dobreva et al. (2005, 2006, 2008) [8, 9, 10], as well as the solar wind-nonmagnetic planet (Venus) interaction Nikolova and Kartalev (1999) [28]. The first application of this numerical methodology in modelling the solar wind-comet interaction was done in the paper of Nikolova and Kartalev (1998) [27]. Some basic numerical results are presented in the [23], concerning in particular the influence of the involved photo-chemical processes on the positions of the key surfaces (outer and inner shock waves and contact surface), formed as a result of the

considered interaction. The used parameters are specified there having in mind the measurements obtained during Halley missions (especially – Giotto mission) in 1986. A satisfactory agreement in the outer interaction regions is also demonstrated in [23].

The developed numerical scheme provides a self-consistent solution for all the regions $\mathcal{A}$, $\mathcal{B}$, $\mathcal{C}$, $\mathcal{D}$, defined in [23] satisfactory, where some numerical results, concerning regions $\mathcal{A}$ and $\mathcal{B}$, based on Giotto mission data (as inputs) were presented. The computational domains in all the presented examples are limited by the radius $x^1 = 120^\circ$. Here, in Section 2, the attention is focused on the "inner" regions $\mathcal{C}$ and $\mathcal{D}$, containing gas with a cometary origin.

2. Inner (cometary gas) regions in the solar wind-Comet Halley interaction

Region $\mathcal{C}$.

The model application in the present paper is focused mainly on this inner shocked region. It is important to study the contribution of the possible physical phenomena to the cometary plasma dynamics in this domain, as well as to the shapes and positions of its boundaries: the inner shock wave and the contact surface.

The following photo- and chemical- reactions, introduced to the model (see [23]) are taken into account in this region:

- Photoionization, described by terms, proportional to S_p in the right-hand sides of the Euler equations. The value of the photoionization rate σ is needed for specifying this process.
- Charge transfer, described by source terms, proportional to S_c and loss terms, proportional to L_c, in the right-hand sides. This reaction is specified by the choice of the reaction rate coefficient q_{ch}.
- Dissociative recombination, described by loss-terms, proportional to L_r. The reaction is specified by determining the reaction rate coefficient α.
- Additional physical process is the ion-neutral frictional force, taken into account by the terms, proportional to I^{fr}. The process is characterized by the frictional coefficient K_{in}.

The specification of all above listed processes assumes also a choice of the value of the total cometary gas production rate Q_o ($Q_o \approx 0.5 \times 10^{30}$ s^{-1} for Comet Halley).

Several cases were examined in order to investigate the problem thoroughly. The processes, included in each of them are presented in Table 1.

Cases	S_p	S_c	L_c	L_r	I^{fr}
Case 1	+	+	+	+	+
Case 2	+	+	+	+	−
Case 3	+	−	−	+	+
Case 4	+	−	−	+	−
Case 5	+	+	+	−	+
Case 6	+	+	+	−	−
Case 7	+	−	−	−	+
Case 8	+	−	−	−	−

Table 1. Considered cases for studying the inner shocked region $\mathcal{C}$. The sign "+" or "–" means inclusion or not of the corresponding term in the right-hand sides of the governing fluid equations in this region

The used values of the character parameters (if there is a plus sign in the corresponding column of Table 1) are $\sigma = 10^{-6}$ s^{-1}, $q_{ch} = 10^{-16}$ cm^2, $\alpha = 7 \times 10^{-8}$ cm^{3}s^{-1}, $k_{in} = 1.1 \times 10^{-8}$ cm^{3}s^{-1}.

One could observe that it is reasonable to separate the introduced cases into two general groups: *Cases 1* ÷ *4*, including dissociative recombination, and *Cases 5* ÷ *8*, without dissociative recombination. There is a correspondence between the cases of these two groups: *Case 1* corresponds to *Case 5*, *Case 2*

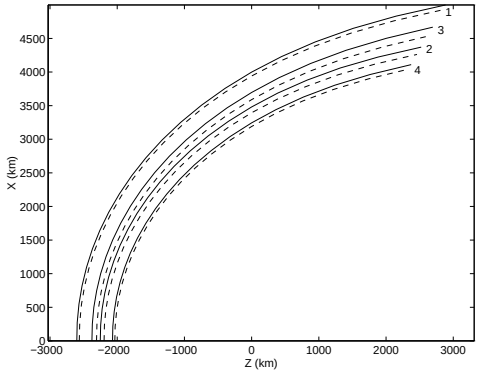

Fig. 1. Obtained shapes of the inner shock waves: Solid lines *1* ÷ *4* correspond to the *Cases 1* ÷ *4*; Dashed lines *1* ÷ *4* correspond to the *Cases 5* ÷ *8*

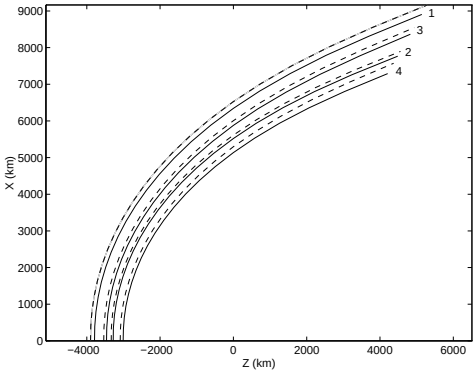

Fig. 2. Obtained shapes of the contact surfaces, marked in analogy with the shocks in Figure 1

– to *Case 6*, *Case 3* – to *Case 7*, *Case 4* – to *Case 8*.

The obtained geometries of the region C for different cases are shown in Figs 1 and 2. The inner shock waves (Fig. 1) for the *Cases 1* ÷ *4* are drawn with solid lines. Each of the inner shocks from the second group *Cases 5* ÷ *8* is situated near to the corresponding shock of the first group and is marked by dashed line. The contact surfaces are drawn in analogical way in the Fig. 2.

A cardinal difference between the introduced two groups of cases appears in the density distribution in the region C. When the dissociative recombination terms are omitted (*Cases 5* ÷ *8*), the density distribution is like that, obtained by Baranov and Lebedev (1988) [2]: the density increases with the cometocentric distance. Such a density behaviour in *Case 8* is demonstrated in Fig. 3. It is worth to recall that a similar density variation contradicts to the experimentally observed density decreasing with this distance (e.g. Balsiger et al. (1986) [1]), Cravens (1986) [6]).

All the cases of the first group, where the dissociative recombination is taken into account, lead to a density distribution, which is in accordance with the experimentally obtained by Giotto instruments – the density generally

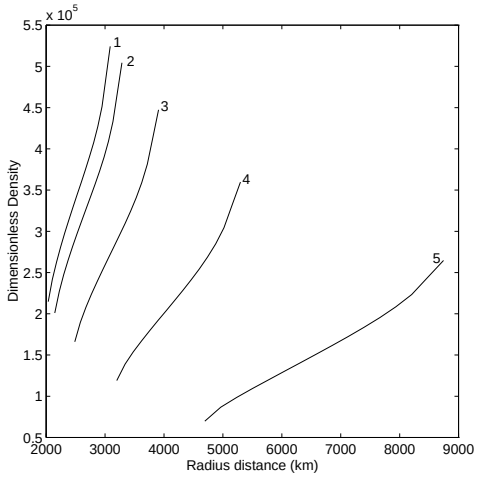

Fig. 3. Numerically obtained density distribution for the *Case 8* in the region C between the inner shock and the contact surface. The curves *1* ÷ *5* present the density distribution along radii at angles $x^1 = 0°, 30°, 60°, 90°, 120°$

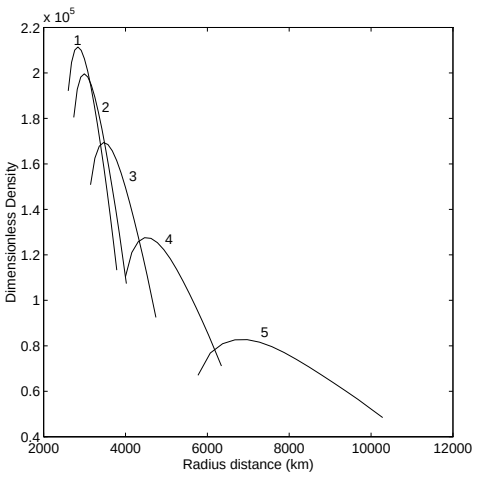

Fig. 4. Numerically obtained density distribution for the *Case 1* in the region C between the inner shock and the contact surface. The curves *1* ÷ *5* present the density along radii containing angles $x^1 = 0°, 30°, 60°, 90°, 120°$ correspondingly. $M^{in} = 1.8$

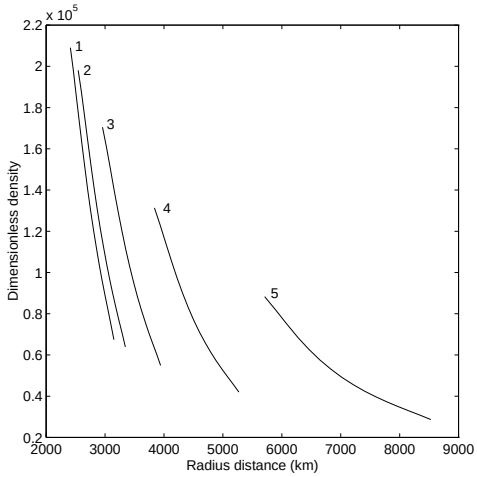

Fig. 5. Numerically obtained density distribution for the *Case 1* in the region C between the inner shock and the contact surface for Mach number of preshock cometary plasma $M^{in} > 4$. The curves $1 \div 5$ present the density along radii: $x^1 = 0°$, $30°$, $60°$, $90°$, $120°$

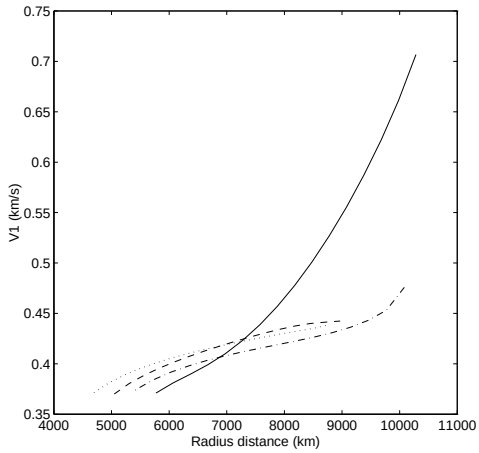

Fig. 6. Distribution of the x^1 component of the velocity (perpendicular to the radial direction) along the radius at angle $x^1 = 120°$ from the sun-comet line. The solid line is for the *Case 1*. The dashed line is for the *Case 6*. The dotted line is for the *Case 8*. The dashdot line is for the *Case 7*

decreases with the cometocentric distance. An example of such a behaviour (for the *Case 1*) is presented in Fig. 4. The Mach number of the pre-shock cometary plasma in this case is $M^{in} = 1.8$.

The density variations for Mach numbers $M^{in} > 4$ along radial directions become monotonically decreasing for all the region C. This is demonstrated in Fig. 5.

As one could expect, the observed differences in the density distribution appear to be in accordance with corresponding differences in the plasma dynamics in the region C. The rate of the "flowing" of the fluid "tailward" is characterized by the x^1 velocity component (which is perpendicular to the radial one). The distribution of this velocity component along the radius at angle $x^1 = 120°$ for different cases is presented in Fig. 6. One can observe much more intensive tailward flow in the *Case 1* in comparison with the *Cases 6, 7, 8*. The velocity distribution in the remaining cases with dissociative recombinations is very much similar to that of the *Case 1*.

The patterns of the Mach number isolines for the *Case 1* are presented

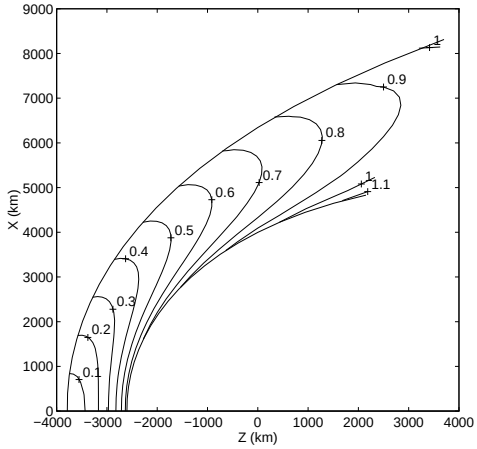

Fig. 7. Mach number isolines obtained in the *Case 1*

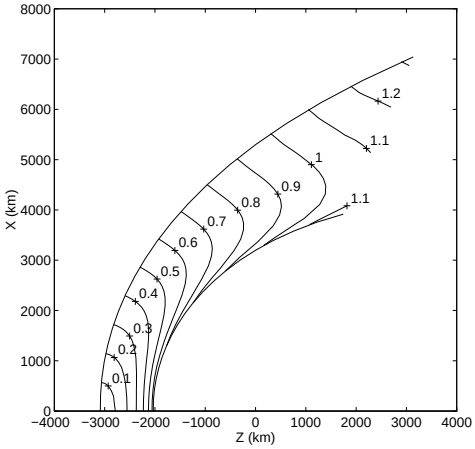

Fig. 8. Mach number isolines obtained in the region C for the *Case 8*, similar to those of the *Cases 5, 6, 7*

in Fig. 7. Similar patterns are obtained for the *Cases 2, 3, 4.*

Another kind of patterns for the Mach number isolines, obtained for the *Cases 5, 6, 7, 8*, is demonstrated in Fig. 8.

The pressure distribution in the *Case 1*, generally typical for all the cases, is drawn in Fig. 9.

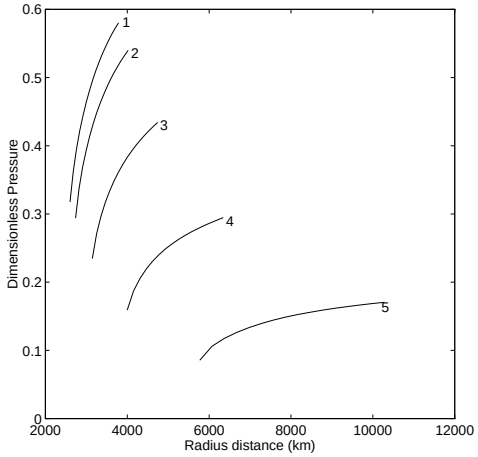

Fig. 9. Distribution of the dimensionless pressure ($p/\rho_\infty V_\infty^2$) along the radii $x^1 = 0°$, 30°, 60°, 90°, 120°. These numerical results, revealed in the *Case 1*, are characteristic for all the other cases

Cases	1	2	3	4	5	6	7	8
IS (km)	4605	4269	4282	4000	4539	4197	4249	3949
CD (km)	7716	7148	7200	6686	7984	7268	7310	6915
OS ($\times 10^6$ km)	1.15	1.15	1.15	1.15	1.15	1.15	1.15	1.15

Table 2. The cometocentric distances of the crossings of the inner shock wave (IS), the contact surface (CD), and outer shock (OS) with the radius, shifted at 108° from the comet-sun line. This radius approximately matches the Giotto trajectory

It seems to be quite important to analyze the crossings of this surfaces with radius, shifted from comet-sun line at about 108° considering the obtained shapes and positions of the shocks and the contact surface. These points are presumably good enough approximations of the crossings of Giotto (or Vega) trajectory with the real discontinuities around comet Halley. The computed for different cases cometocentric distances of these crossings are presented in Table 2.

3. Magnetic cavity boundary in the Halley inner coma: contact surface or inner shock wave?

As noted by Glassmeier et al. (2007) [13], further experimental study of the process of the formation of the cometary magnetic cavity – Neubauer (1987) [26], is amomg the primary scientific targets of the RPS-MAG (Fluxgate magnetometer) team. The magnetic cavity boundary, where the magnetic field drops to zero, plays a crucial role in the inner coma region interpretation. There are some plasma features on this surface, pointing to its interpretation as inner shock. The HIS instrument of the ion mass spectrometer on board the Giotto spacecraft Schwenn et al. [30] identified this surface (called "contact" in that paper) at 4800 km distance from the comet nucleus. This boundary is clearly seen by a drastic drop in the temperatures of different ion species from about 2000 K outside to values, as low as 300 K inside. Also, inside the contact surface an outflow speed of ~ 1 km s^{-1} was measured, in contrast to a value around zero right outside. This is a typical "shock like" behaviour of the radially flowing super-sonic ionized gas with comet a origin. The fact that the interplanetary magnetic field reaches the magnetic cavity boundary, evidently prevents its interpretation as an inner shock. The IMF cannot penetrate through the contact surface (CS) because in the frame of the classic MHD approach.

Kartalev (1998) [17] proposed an introduction of "mass-loading diffusion" which can explain a penetration of the IMF through the CS and its inva-

sion till the inner shock (IS). The cause of this specific magnetic field diffusion is the fact that the picking up of new ions is **a non-instantaneous process**. This process passes three basic stages – Gaffey et al. (1988) [11]: (i) Ring-beam distribution; (ii) Shell – distribution; (iii) Relaxation to a suprathermal distribution. In the first ("fresh ions") stage in the randomization process these ions still have the velocity **w** of the comet neutrals, but they do affect the electromagnetic field: they cause a kind of shielding electric field, which is external to the fluid and, respectively, **effective external charges and currents** appear. As a result, the magnetic field became frozen in a certain virtual fluid possessing virtual bulk velocity **U**:

$$\mathbf{U} = \mathbf{u} - \frac{N_f}{n}\mathbf{w}, \tag{1}$$

where **u** is the velocity of the ambient plasma with density n, **w** is the (radial) velocity of the background collisionless neutral particles flow, and $N_f$is the number density of the substance of the fresh new ions. As a final result, a new term appears in the magnetic induction equation (2), causing a quasi-diffusion of the magnetic field into **direction, opposite to the velocity of the cometary neutrals**:

$$\frac{\partial \mathbf{B}}{\partial t} = [(\mathbf{u} \times \mathbf{B}) - \frac{N_f}{n}\ (\mathbf{w} \times \mathbf{B})]. \tag{2}$$

This new term provides a **magnetic field supplemental convection** against the **w** direction and, respectively, a penetration of the interplanetary magnetic field behind the contact surface, towards the inner shock wave. This is a direction against the radial flow of the cometary neutrals, as well, generally against the flow of the ambient cometary plasma. This is a situation absolutely impossible in the frame of the "classic" ideal MHD. Such penetration was demonstrated by Kartalev and Nikolova (1998b) [18], applying a numerical one-dimensional modelling of the inner coma structure with mass-loading diffusion.

Let consider the region $\mathcal{D}$. As the fresh ions velocity **w** is equal in this collisionless region to the bulk velocity of the ambient plasma **u**, they are picked up instantaneously there, i.e. $N_f = 0$, $\mathbf{U} \equiv \mathbf{u}$. There is, no therefore, a magnetic field supplemental convection in the region $\mathcal{D}$. So, if even the interplanetary magnetic field do penetrate somehow to the boundary, separating regions $\mathcal{D}$ and $\mathcal{C}$ (the inner shock), it couldn't penetrate through this boundary inside into the region $\mathcal{D}$, because the flow in this region is directed outwards, and the magnetic field has to be frozen in (in the classic MHD sense).

Besides the above exposed consideration, we shall present below some additional justifications of our model results: comparisons of measured parameters along Giotto inner coma trajectory and numerical predictions of their distribution. There is a very character experimental result from Giotto mass spectrometer – Balsiger et al. (1986) [1], Cravens (1986) [6]. An interesting segment of the measured density variation in the inner coma is presented by dotted line in Fig. 10: The plasma density is decreasing outwardly from the magnetic cavity boundary, placed at 4700 km from the comet nucleus (point C in Fig. 10). Then, there is a density peak at a distance about 6800 $\div$ 10000 km. (again along the Giotto trajectory). Going farther from the nucleus, the density continues to decrease monotonically. We do not know any preceding model studies, where the obtained numerically density behaviour corresponds satisfactorily to the mentioned character variations of the density distribution.

Density distribution over the same segment consider our picture of the numerically obtained for the *Case 1*, along the radius is $x^1 = 108^\circ$ (resembling Giotto trajectory). Our results are drawn in Fig. 10 by solid line. The vertical dotted lines are marking our predictions of the inner shock and of the contact discontinuity. One can observe a coincidence between our inner shock and the magnetic cavity boundary. The position of our contact surface is near the point of the sharp peak of the experimental density (point A). The segment AB of the experimental density variation could be interpreted as a structure of the real contact surface. In our idealized consideration this surface is approached by a jump (infinitesimally thin discontinuity). The tendency of the computed density variation is exactly as that given from the experiment. The computed by Baranov and Lebedev (1988) [2] density profile for the same segment is plotted by dash-dotted line in Fig. 10 for comparison with earlier obtained theoretical results. The data are taken from Fig. 12 of their paper. The points B_i and B_c are the predicted by these authors inner shock and contact surface, correspondingly. Note that the presented curve of Baranov and Lebedev (1988) [2] in our terminology corresponds to the radius $x^1 = 90^\circ$. So, the positions of the considered discontinuities could be even at larger cometocentric distances for the radius $x^1 = 108^\circ$.

Some comments are required about the observed in Fig. 10 lack of substantial density jump in the experimental data (point C). It could be explained by the fact that the presented here result is from the original data analysis, which are supposed to be inadequate due to a low spatial resolution – Cravens (1991) [7]. A density enhancement among a factor of 3.5 and 20 was obtained

by more precise data analysis.

It is interesting to consider the numerically obtained temperature distribution along the same segment, analyzed in Fig. 10. The numerically obtained here temperature distribution solid line in Fig. 11 is in a satisfactory agreement with the experimentally obtained one, presented by the dashed line in Fig. 11 – Gombosi et al. (1996) [14]. Note that the latter distribution is introduced as an **external to the model** information there! This temperature distribution is causing the obtained by Gombosi et al. (1996) [14] density distribution, matching the experimental one. In our model, approximation everything is a "natural" consequence of the self-consistent flow dynamics.

The region between the magnetic cavity and the density peak is not now "prohibited" to be an inner shocked region taking into account the possible "mass-loading magnetic field diffusion". So, one can conclude that there are quite reliable reasons (for the *Cases 1 ÷ 4*) for interpretation of the magnetic cavity boundary as an inner shock and the discussed density peak as a contact discontinuity.

Note that the interpretation of the "pile-up" region – the domain of sharply density increasing between $\sim 1.4 \times 10^5$ km and $\sim 10^4$ km is in fact also in good agreement with the so proposed interpretation: This is exactly the inner segment of the region B in our consideration, where the density sharply increases (Figs 10 and 5 from [23]).

The numerically achieved positions of the three discontinuities along the radius $x^1 = 108^\circ$ are summarized in Table 2. The positions of the inner shock and the contact surface depend slightly on the values of the parameters, specifying the mass-source and mass-loss processes and the frictional force. A common tendency is retained nevertheless: The inner shock and the contact surface are near to the discussed positions for the *Case 1*. Certainly, their positions depend on the choice of the physical parameters, specifying the source-, the loss- processes and the frictional force.

4. Possible scenarios of solar wind-Comet 67P/CG interaction during Rosetta mission. Is the single-fluid model applicable?

Rosetta mission is the next bold step in the huge successes in the direct comet investigations, reached during the recent decades: fly through their comas as in the Giotto and Vega missions to 1P/Halley and the Giotto extended mission to 26P/Grigg-Skjellerup; traverse their tails as on the ICE mission to 21P/Giacobini-Zinner; photograph the nucleus, as on the Stardust mission to 81P/Wild 2, and return a sample of cometary dust; or even excavate a crater,

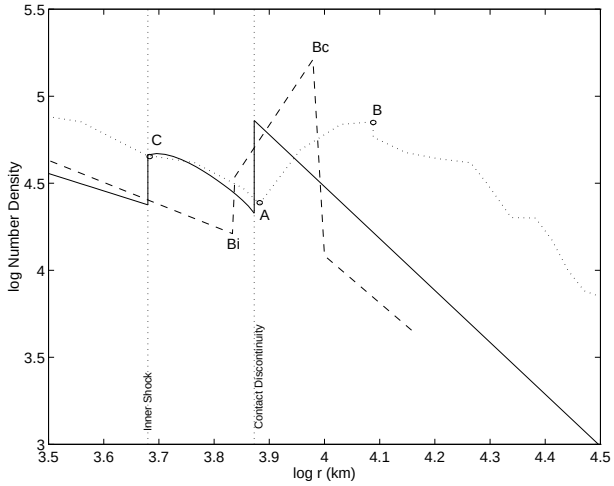

Fig. 10. Density distribution for a segment of the inner coma region. The dotted line is the measured density variation along the Giotto trajectory, taken from Fig. 2 of the paper of Cravens (1986) [6]. The point C is the magnetic cavity boundary. The solid line is our density distribution along the radius $x^1 = 108°$ for the *Case 1.* The vertical dotted lines are marking the predicted by our consideration positions of the inner shock and the contact surface. The dash-dotted line presents the computed by Baranov and Lebedev (1988) [2] density variation along the radius $x^1 = 90°$ (Fig. 8 there). The points B_i and B_c are the predicted by these authors inner shock and contact surface

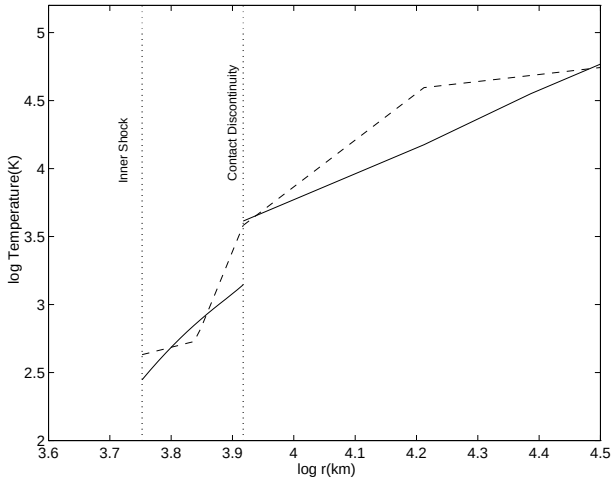

Fig. 11. Numerically obtained temperature distribution along the same segment as in Fig. 10 (solid line). The dashed line presents the *given* temperature distribution in the paper of Gombosi et al. (1996) [14]

such as on the Deep Impact mission to 9P/Tempel 1. The Rosetta lander module, however, will perform a pioneering landing on a comet; meeting it on its own surface; and decoding the record written on its surface. Besides this, for the first time in the comet exploration history, the Rosetta Comet Rendezvous Mission will provide a unique opportunity to study a cometary environment and its interaction with the solar wind over a wide range of distances from the Sun, hence a wide range of activity levels. Rosetta will first encounter the comet when it is relatively dormant, at a heliocentric distance of greater than 3 AU, and will follow the comet to perihelion at approximately 1 AU over a period of one year.

The instrument complex GIADA (Grain Impact Analyser and Dust Accumulator) [5] will be plunged in the dust environment of the coma and will be able to explore dust flux evolution and grain dynamics properties with position and time. This will represent a unique opportunity to perform measurements on key parameters that no ground-based observation or fly-by mission is able to obtain and that no tail or coma model elaborated so far has been able to properly simulate. The characterisation of dust abundance and dynamics is needed to: (a) shade light on dust emission processes from nucleus, (b) understand coma evolution and (c) clarify dust-gas relations.

The Rosetta Plasma Consortium (RPC) instruments [3, 4, 13] have been designed to measure the fundamental parameters of the plasma environment over the wide dynamic range which will be encountered during the mission. It is supposed that RPC will study the interaction of the magnetised solar-wind plasma with the comet, and in particular will observe the dynamics and evolution of the interaction region as the comet activity increases.

Several ***scenarios*** are foreseen in studying the comet environments [4]:

1. ***Large heliocentric distances.*** Distances typically > 2 AU. The nucleus is un-shielded. The solar wind directly impacts the nucleus surface. Energetic pick-up ions can also reach the surface.
2. ***Intermediate scales.*** The developing coma shields the nucleus from the solar wind, but a fully thermalised plasma environment has yet to develop. ***The Rosetta spacecraft will orbit the comet at distances of some tens of km within the developing coma.***
3. ***Perihelion scales.*** Distances, typically < 1.5 AU. A thermal plasma region of some hundreds of km in size shields the nucleus from the solar wind and a diamagnetic cavity of the order 10's km forms, bounded by the contact surface. (The plasma team expects – Carr et al. (2007) [4] that Rosetta spacecraft, orbiting the comet, will be inside the contact

surface.)

4. ***The plasma tail.*** Excursions of up to 104 km from the nucleus are planned, depending on the fuel resources. In an extended mission, Rosetta may make in-situ measurements of the tail at distances to 104 km (suggested; not part of the nominal mission).

It is worth noting that the operation "Rosetta orbit around the comet" has some peculiarities [24]for better understanding the possible capabilities of the investigations' planning: The comet is a comparatively small body with a radius, estimated at 2.5 km. In a typical orbit, its gravitational attraction is about the same order of magnitude as the solar and planetary perturbations and the solar radiation pressure. This means that the spacecraft will not fly on Kepler orbits. It will also be difficult to predict the precise position of the spacecraft for more than a few days to weeks in advance. Thus, a concept based on e.g. a "frozen orbit", used in many other planetary missions, cannot be used. In particular, the pointing timeline for the spacecraft will need to be schedulable in a very flexible way, e.g. based on events, and it must be possibly to change it quite late in the planning cycle. Another obvious issue when preparing a planning concept for a comet is the fact that the comet will change as it gets closer to the Sun: It will become more active and additional perturbing forces on the spacecraft due to volatiles emanating from the comet's nucleus will increase. Also, dust jets may become active on the nucleus which would need to be avoided by the spacecraft.

The above note determines the great importance of modelling the operational management of the whole project. Practically, continuous models' running could be required, applying as inputs currently measured data values. This may give guidance for specifying the next orbiter trajectory parameters, as well as instruments' operational modes.

As to the model considered here, it needs as inputs solar wind parameters and the parameters of the collisionless outflow (if it exists) of the cometary neutrals (as well the characteristics of the process of their ionization). The creation mechanisms of these outflow particles around the comet nucleus was discussed from the very early papers on the topic. Thus, Wallis and Dryer (1976) [32] found that there is an innermost subsonic flow upstream of the comet source that undergoes upstream transition to supersonic flow. They cited Probstein (1968) [29] who showed that a drag of a dust component gives a transition from subsonic to supersonic expansion, at a distance above the source surface of order (ρ_{dust}/ρ_{gas}) times the dust grain diameter. Modelling complicated processes in the near-comet vicinity underwent substantial

development and many sophisticated state-of-the-art models will be applied in the interpretation of the GIAGA experiments (see Colangeli et al. (2007) [5] and the bibliography therein), providing in particular appropriate input data to the models, describing solar wind-comet interaction.

It should be different in each of the above mentioned scenarios as regard to the possible utilization of our model:

Scenario 1. Large heliocentric distances. No substantial implementation of the present model. It could be interesting from the point of view of the solar wind-comet interaction to check up if the Orbiter magnetometer will register just the IMF, or some electromagnetic interaction with the conducting comet body will take place.

Scenario 4. The plasma tail. The present model is not applicable to this region in the existing now stage. Its extension to the comet tail region is possible in the frame of the same mathematical approach.

Scenario 3. Perihelion scales. This is exactly the case, considered in the present model and found experimentally by Giotto and Vega spacecrafts around Comet Halley. Most distinct feature of this case is the existing of the inner shock wave. The magnetometer should detect zero magnetic field (magnetic cavity) according to the presented above (in Section 3) consideration even if the Rosetta Orbiter doesn't cross the inner shock because of a very low orbit. A good idea in such a case could be to schedule an appropriate short Orbiter excursion in Sun direction – trying to cross the inner shock and the contact surface.

Scenario 2. Intermediate scales. Here, we have in mind the case, when the cometary gas outflow is not able to reach a supersonic stage (but undergoes ionization, as in the Case 3!). This may happen because of a too low gas production rate, specific solar wind conditions, or specifics of the near-comet processes. *Scenario 2* should arise necessarily when the comet is near enough to the perihelion while it is possible that *Scenario 3* could not be reached during the mission for some reason. We will consider this case in details elsewhere. Here, we will mention only the fact, that this case resembles very much the picture of the solar wind flow around the non-magnetic planet with extensive exosphere – like Venus – Nikolova and Kartalev (1999) [28]. It is also worth mentioning that, like in the case of Venus Kartalev (1998) [19], the magnetic field supplemental convection, considered in Section 3, causes IMF penetration behind the contact surface. Let us remind that here the inner shock is missing. The ionized comet outflow is deflected from its radial direction, being forced to "wrap" an obstacle (contact discontinuity). In this

case a draped (behind the CS) IMF is expected to penetrate inside, filling all the region, containing ionized cometary gas. This draped IMF could be registered by Orbiter magnetometer.

5. Summary and discussion

Furthermore, results about inner coma region are demonstrated and discussed utilizing the presented in the accompanying [23] numerical single-fluid model of the comet exosphere-solar wind interaction. The dependence of the region structure and parameters' distribution on the inclusion of different photochemical processes in the Euler system of equations is studied. The best model "tuning" is obtained, corresponding to the satisfactorily accordance with Giotto measurements around P/Halley. A very good coincidence is obtained between some parameters variation along Giotto trajectory and predicted by the model ones. The earlier proposed by Kartalev (1998) [17] "supplemental magnetic diffusion" concept, based on a specific magnetic diffusion in mass-loaded plasma, is implemented. As a result, magnetic field penetration behind contact surface is explained and re-interpretation of the magnetic cavity boundary as an inner shock wave is obtained. This revelation is supported by Giotto measurements too. Possible utilization of the model in future Rosetta data interpretation is discussed for each of the planned mission stages. Especially effective could be this contribution for the *Intermediate and Perihelion scales Scenarios*, where the model should be useful even in the operative project scheduling activities.

REFERENCES

[1] Balsiger, H., K. Altwegg, F. Buhler, J. Geiss, A. G. Ghielmetti, B. E. Goldstein, R. Goldstein, W. T. Huntress, W.-H. Ip, A. J. Lazarus, A. Meier, M. Neugebauer, U. Rettenmund, H. Rosenbauer, R. Schwenn, R. D. Sharp, E. G. Shelley, E. Ungstrup, D. T. Young. Young Ion Composition and Dynamics at Comet Halley. *Nature*, **321** (1986), 330–334.

[2] Baranov, V. B., M. G. Lebedev. Solar-wind Flow Past a Cometary Ionosphere. *Astrophysics and Space Science*, **147** (1988), 69–90.

[3] Burch, J. L., R. Goldstein, T. E. Cravens, W. C. Gibson, R. N. Lundin, C. J. Pollock, J. D. Winningham. RPC-IES: The Ion and Electron Sensor of the ROSETTA Plasma Consortium. *Space Science Reviews*, **128** (2007), 697–712.

[4] Carr, C., E. Cupido, C. Lee, A. Balogh, T. Beek, J. Burch, C. Dunford, A. Eriksson, R. Gill, K. Glassmeier, R. Goldstein, D. Lagoutte, R. Lundin, K. Lundin, B. Lybekk, J. Michau, G. Musmann, H. Nilsson, C. Pollock, I. Richter, J. Trotignon. RPC: The ROSETTA Plasma Consortium. *Space Science Reviews*, **128** (2007), 629–647.

[5] Colangeli, L., J. J. Lopez-Moreno, P. Palumbo, J. Rodriguez et al. The Grain Impact Analyzer and Dust Accumulator (GIADA) Experiment for the ROSETTA Mission: Design, Performances and First Results. *Space Science Reviews*, **128** (2007), 803–821.

[6] Cravens, T. E. The Physics of the Cometary Contact Surface, In ESA Proceedings of the 20th ESLAB Symposium on the Exploration of Halley's Comet. Volume 1: Plasma and Gas, (1986), 241–246.

[7] Cravens, T. E. Plasma Processes in the Inner Coma, In: Comets in the post-Halley era, Vol. **2** (Eds R. L. Newburn, Jr., M. Neugebauer and J. Rahe), MA, Norwell, Kluwer Academic Publishers, 1991, 1211–1255.

[8] Dobreva, P. S., M. D. Kartalev, N. N. Shevyrev, G. N. Zastenker. Comparison of a New Magnetosphere-magnetosheath Model with Interball-1 Magnetosheath Plasma Measurements. *Planetary and Space Science*, **53** (2005), 117–125.

[9] Dobreva, P., M. Kartalev, N. Shevyrev, G. Zastenker, A. Koval. Interpretation of Satellite Magnetosheath Plasma Measurements using Magnetosheath-magnetosphere Numerical Model. *Journal of Theoretical and Applied Mechanics*, **36** (2006), No. **3**, 3–16.

[10] Dobreva, P. S., M. D. Kartalev, D. Koitchev, V. I. Keremidarska, M. Kaschiev. On the Modular Approach of a 3D Model of the System Magnetosheath-magnetosphere. *Journal of Advances in Space Research*, **41** (2008), No. **8**, 1279–1285.

[11] Gaffey, Jr. J. D., D. Winske, C. S. Wu. Time Scales for Formation and Spreading of Velocity Shells of Pickup Ions in the Solar Wind. *J. Geophys. Res*, **93** (1988), No. **A6**, 5470–5486.

[12] Glassmeier, K. H., H. Boehnhardt, D. Koschny, E. Kuhrt, I. Richter. The ROSETTA Mission: Flying towards the Origin of the Solar System. *Space Sci. Rev.*, **128** (2007), 1–21.

[13] Glassmeier, K. H., I. Richter, A. Diedrish, G. Musmann et al. RPC-MAG The Fluxgate Magnetometer in the ROSETTA Plasma Consortium. *Space Science Reviews*, **128**, (2007), 649–670.

[14] Gombosi, T. I., D. L. De Zeeuw, R. M. Haberli, K. G. Powell. Three-dimensional Multiscale MHD Model of Cometary Plasma Environments. *J. Geophys. Res.*, **101** (1996), No. A7, 15233–15253.

[15] Hansen, K. C., T. Bagdonat, U. Motschmann, C. Alexander, M. R. Combi, T. E. Cravence, T. I. Gombosi, Y.-D. Jia, I. P. Robertson. The

Plasma Environment of Comet 67P/Churyumov-Gerasimenko throughout the Rosetta Main Mission. *Space Science Reviews*, **128** (2007), 133–166.

[16] Kartalev, M. D., V. I. Nikolova, V. F. Kamenetsky, I. P. Mastikov. On the Self-consistent Determination of Dayside Magnetopause Shape and Position. *Planet. Space Sci.*, **44** (1996), 1195–1208.

[17] Kartalev, M. D. On the Single-Fluid Modelling of Mass-loaded Plasma. *Geophys. Astrophys. Fluid Dynamics*, **88** (1998), 131–164.

[18] Kartalev, M. D., V. I. Nikolova. On the Magnetic Field Diffusion in MHD Modelling of the Inner coma of Comet Halley. *Geophys. Astrophys. Fluid Dynamics*, **89** (1998), 145–168.

[19] Kartalev, M. D. Diffusion of the Interplanetary Magnetic Field into the Planetosphere of Venus. *J. Theor. Appl. Mech.*, **28**, (1998), No 4, 51–61.

[20] Kartalev, M. D., V. I. Keremidarska, K. G. Grigorov, D. K. Romanov. Near Real Time Determination of the Manetopause and Bow Shock Shape and Position, In: ESA SP-477, Noordwijk: ESA Publications Division, 2002, 555–558.

[21] Kartalev, M., S. Savin, E. Amata, P. Dobreva, G. Zastenker, N. Shevyrev. Magnetopause Cusp Indentation: an Attempt for a New Model Consideration, In Proc. of: Cluster and Double Star Symposium, 5th Anniversity of Cluster in Space, ESA SP-598, ESA Publications Division, 2006, 29.

[22] Kartalev, M., P. Dobreva, E. Amata, M. Dryer, S. Savin. Some Tests ot a New Magnetosheath Model via Comparison with Satellite Measurement. *Journal of Atmospheric and Solar-Terrestrial Physics*, **70** (2008), 627–636.

[23] Keremidarska, V., M. Kartalev, P. Dobreva, M. Dryer. Solar Wind-comet Exosphere Interaction. 1. A Single Fluid Gasdynamic Model. *Journal of Theoretical and Applied Mechanics*, **41** (2011), No. 3, 65–82.

[24] Koschny, D., V. Dhiri, K. Wirth, J. Zender, R. Solaz, R. Hoofs, R. Laureijs, T.-M Ho, B. Davidsson, G. Schwehm. Scientific Planning and Commanding of the ROSETTA Payload. *Space Science Reviews*, **128** (2007), 167–188.

[25] Magomedov, K. M., A. S. Holodov. Grid Characteristic Numerical Methods, Moscow, Nauka, 1988.

[26] Neubauer, F. M. Giotto Magnetic-field Results on the Boundaries of the Pile-up Region and the Magnetic Cavity. *Astron. Astrophys.*, **187** (1987), 73–79.

[27] Nikolova, V. I., M. D. Kartalev. Numerical Grid-characteristic Modelling of the Solar Wind Flow Around Comets, Finite Difference Methods: Theory and Applications, (Eds A. A. Samarskii et al.), Commack, USA, NY, Nova Science Publishers, 1998, 197–205.

[28] Nikolova, V., M. Kartalev. On the Numerical Modelling of the Venus Planetosphere/Mantle. *J. Theor. Appl. Mech.*, **29** (1999), No. **1**, 56–68.

[29] Probstein, R. F. The Dusty Gasdynamics of Comet Heads, In: Problems of Hydromechanics and Continuum Mechanics, (Ed. M.A. Lavrentiev), Philadelphia, Society for Industrial and Applied Mathematics, 1968.

[30] Schwenn, R., W.-H. Ip, H. Rosenbauer, H. Balsiger et al. Ion Temperature and Flow Profiles in Comet P/Halley's Close Environment. *Astron. Astropys.*, **187** (1987), 160–162.

[31] Trotignon, J. G., R. Bostrom, J. L. Burch, K. H. Glassmeier, R. Lundin, O. Norberg et al. The ROSETTA Plasma Consortium: Technical Realization and Scientific Aims. *Advances in Space Research*, **24** (1999) 1149–1158.

[32] Wallis, M. K., M. Dryer. Sun and Comets as Sources in an External Flow. *The Astrophysical Journal*, **205** (1976), 895–899.

[33] Zapryanov, Z. D., V. B. Minostsev. Method of Calculating Three-dimensional Supersonic Gas Flows around Bodies, In: Izv. AN SSSR, Mehanika i Mashinostroenie, **4** (1964), 20–24, (in Russian).